PENERBIT
USM

THEORETICAL INVESTIGATION AND DESIGN OF BIOACTIVE QUINOLINE DERIVATIVES AS INHIBITORS OF DNA GYRASE OF *SALMONELLA TYPHI*

JOHN PHILIP AMEJI[1*], ADAMU UZAIRU[2], GIDEON ADAMU SHALLANGWA[2] AND SANI UBA[2]

[1]Department of Chemistry, Federal University Lokoja, Kogi State, Nigeria
[2]Department of Chemistry, Ahmadu Bello University, Kaduna State, Nigeria

ABSTRACT

The ever-increasing rate of resistance to existing antibiotics by Salmonella typhi has made the search for novel drug candidates a necessity. In this study, Molecular docking technique was used to screen 18 bioactive quinoline derivatives against DNA gyrase of Salmonella typhi using PyRx graphical user interface of AutoDock Vina software. Ligand with the best binding affinity against the target macromolecule was used as prototype to design novel analogues with enhanced potencies. With the aid of Swiss ADME online server and Osiris DataWarrior v5.5.0 programme, the absorption, distribution, metabolism, excretion and toxicity (ADMET) profiles of the ligands were evaluated and their electronic properties were computed using density functional theory (DFT) method of Spartan 14.0 software. Ligand 3 (L3) with the best binding affinity (ΔG) value of −10.5 kcal/mol was chosen as a prototype to design La and Lb with ΔG value of −10.7 kcal/mol and −10.8 kcal/mol; binding constant (k_a) of 7.04×10^7 and 8.35×10^7; and dissociation constant (k_d) of 1.42×10^{-8} and 1.2×10^{-8}, respectively. When compared with ciprofloxacin ($\Delta G = −7.7$ kcal/mol), the ligands could be more potent. Likewise, the ligands were found to possess excellent oral bioavailability and pharmacokinetic profiles. Furthermore, DFT calculations on La and Lb revealed that they possess highest occupied molecular orbital-lowest unoccupied molecular orbital (HOMO-LUMO) energy gap of 3.46 eV and 3.45 eV; and global electrophilicity index of 3.83 eV and 3.96 eV, respectively. The designed ligands tend to be consistent with all the validation protocols deployed in this study and as such could be recommended as novel drug candidates for treatment of Salmonella typhi induced salmonellosis.

Keywords: *Quinoline, Salmonella typhi, DNA gyrase, HOMO, LUMO*

*Corresponding author: ameji4real55@gmail.com

INTRODUCTION

Theoretical chemistry explains the structures and dynamics of chemical systems by encapsulating the ideas of quantum mechanics, classical mechanics and statistical mechanics. Theoretical chemistry concepts well incorporated into efficient computer programme known as computational chemistry, has found immense applications in modern drug discovery and design strategies. Research has shown that the development of new drug from target discovery to drug registration could gulp up to USD2 billion and 10–17 years, making drug discovery and development a time-consuming, energy-sapping and extremely capital expensive venture (Leelananda and Lindert 2016). However, the application of methods of theoretical chemistry, known as computer aided drug design (CADD) has been able to mitigate the aforementioned challenges. CADD techniques have been successfully applied in the development of some novel drugs such as captopril, dorzolamide, saquinavir, zanamivir, oseltamivir, aliskiren, boceprevir, nolatrexed, TMI-005, LY-517717, rupintrivir and NVP-AUY922, many of which have either been approved or in clinical trials (Talele *et al*. 2010; Sliwoski *et al*. 2013; Devi *et al*. 2015; Nunes *et al*. 2019).

A cardinal technique in a CADD is the molecular docking based virtual screening. This technique is used to predict the binding interaction between a data base of bioactive molecules (ligands) and the active sites of a known macromolecular target (receptor). The most promising ligands are the ones which form the most stable complex with the receptor based on their binding affinity to the target (Liu *et al*. 2018). This technique has attracted wide patronage in recent years owing to its fast and cost effectiveness in screening data base of bioactive ligands (Carregal *et al*. 2017; Mugumbate *et al*. 2017; Wójcikowski *et al*. 2017; Carpenter *et al*. 2018; Dutkiewicz and Mikstacka 2018; Surabhi and Singh 2018; Nunes *et al*. 2019). In addition to identification of bioactive leads, virtual screening technique also assists in lead optimisation processes (i.e. transformation of leads into more effective and efficient drug candidates by improving their pharmacophores). The optimised leads are then subsequently subjected to clinical and preclinical trials before been approved as drugs by appropriate regulatory agencies (Lima *et al*. 2016).

In the binding of ligands (L) to protein target (P) to form ligand-protein complex (LP), L and P constitute the reactants while LP constitutes the product. The reaction is represented by Equation 1.

$$L + P \underset{k_d}{\overset{k_a}{\rightleftharpoons}} LP \qquad\qquad \text{Equation 1}$$

where k_a and k_d are the binding and dissociation constants, respectively. These two constants are related by Equation 2 at equilibrium.

$$k_a = \frac{[LP]}{[L][P]} = \frac{1}{k_d} \qquad\qquad \text{Equation 2}$$

[*LP*] in Equation 2 represents the concentration of the LP complex while [*L*] and [*P*] give the concentrations of the ligand and the protein target, respectively.

The reaction in Equation 1 could be likened to a thermodynamic system in which L and P which constitutes the solutes undergo complex reactions and heat exchange with the solvent (i.e. water) and the buffer ions in the biological system. The standard Gibb's free energy change (ΔG^0) of the LP interaction is expressed by Equation 3.

$$\Delta G^0 = -k_B T \ln\left(C^0 k_a\right)$$

Equation 3

where, $R = N_A \times k_B$, where, N_A, k_B, R, T and C^0 are the Avogadro's constant (6.022×10^{23}), Boltzmann's constant (1.38×10^{-23} J/K), universal gas constant ($R = 8.314$ Jmol^{-1}K^{-1}), absolute temperature and standard concentration of 1M for all reacting molecules, respectively. The negative value of ΔG^0 varies directly with the thermodynamic stability of the LP complex (Limongelli 2020).

A very useful expression of ΔG^0 in terms of chemical potential (μ) has also been provided by statistical mechanics as shown by Equation 4.

$$\Delta G^0 = \mu_{LP} - \mu_L - \mu_P = -k_B T \ln\left[\frac{C^0}{8\pi^2}\frac{\int e^{-(\mu_{rLP})+\left(\frac{S_{rLP}}{K_B T}\right)}\,dr\,(LP)}{\left(\int e^{-(\mu_{rL})+\left(\frac{S_{rL}}{K_B T}\right)}\,dr\,(L)\right)\left(\int e^{-(\mu_{rP})+\left(\frac{S_{rP}}{K_B T}\right)}\,dr\,(P)\right)}\right]$$

Equation 4

where, μ_{LP}, μ_L and μ_P are the potential energy of the complex, ligand and protein, respectively. The factors rLP, rL and rP represent their corresponding internal coordinates (or conformations), while S_{rLP}, S_{rL} and S_{rP} give their solvation energy values. The rotational degree of freedom of LP, L and P are accounted for by the $8\pi^2$ factor.

Furthermore, it is pertinent to note that the interaction of ligands with the active sites of the macromolecule is dynamic and not static. Hence, the kinetic investigation of the LP complex in a mechanically perturbed system is sacrosanct. From Equation 2, if a ligand binds to a macromolecular target such that $k_a > k_d$, such ligand is considered to possess favourable kinetic stability and could be regarded as promising drug candidate (Limongelli 2020).

Another key factor worthy of note in a drug candidate is its ability to withstand both physical and chemical degradation. This unique property is influenced by energies of the frontier molecular orbitals comprising of the highest occupied molecular orbital (HOMO) and the lowest unoccupied molecular orbital (LUMO). In the course of chemical reaction, the HOMO donates electron and the LUMO accepts electron. The energy difference (energy gap) between these orbitals computed using Equation 5 determines the kinetic stability of molecules while the global electrophilicity index (ω) descriptor calculated using Equation 6 influences their thermodynamic stabilities. Higher energy gap implies low chemical reactivity and excellent kinetic stability while higher ω value in a molecule implies its strong electrophilic behaviour (Srivastava 2021).

$$\Delta E \text{ (energy gap)} = E_{LUMO} - E_{HOMO}$$

Equation 5

where E_{LUMO} and E_{HOMO} represents the energy of LUMO and HOMO, respectively.

$$\omega = \frac{\mu^2}{2\eta}$$

Equation 6

where η is the global chemical hardness expressed in Equation 7 and μ the electronic chemical potential defined in Equation 8.

$$\eta = \frac{E_{LUMO} - E_{HOMO}}{2} \qquad \text{Equation 7}$$

$$\mu = \frac{E_{LUMO} + E_{HOMO}}{2} \qquad \text{Equation 8}$$

Another important CADD technique is the pharmacokinetic and toxicity profiling of drug candidates at the early stage of drug discovery and development. At this stage, the fate of the therapeutic molecules in the biological system is ascertained through the prediction of their absorption, distribution, metabolism, excretion and toxicity (ADMET). This helps to lower possible attrition rate at the late stage of drug development (Ameji *et al.* 2022; Ameji *et al.* 2023a; 2023b; 2023c).

Quinolines constitute a class of natural mixtures of aromatic heterocyclic series comprising of a benzene ring fused to a pyridine ring at two neighbouring carbon atoms. They possess a wide spectrum of pharmacological activities such as antibacterial, anti-tumour, anti-inflammatory and anti-microbial effects (Behforouz *et al.* 2017; Gholizadeh and Radmoghadam 2014; Kumar *et al.* 2010). The profound therapeutic potentials inherent in quinoline nucleus has made them essential components of many approved drugs such as nalidixic acid, ciprofloxacin, levofloxacin, norfloxacin, etc. (Behera *et al.* 2022).

DNA gyrase which is the macromolecular target in this study, is a type II topoisomerase that relax supercoiled DNA and introduces negative supercoiling in DNA during replication in a reaction involving hydrolysis of adenosine triphosphate (ATP) (Bates and Maxwell 2007). Therapeutic compounds targeting DNA gyrase function by either inhibiting its enzymatic activity (ATPase activity) or stabilising the covalent enzyme-DNA complex formed (gyrase poisoning) during replication, creating room for series of events that will result in cell death (Drlica *et al.* 2009; Kohanski *et al.* 2007).
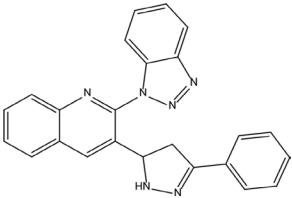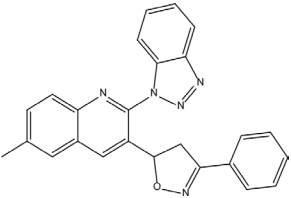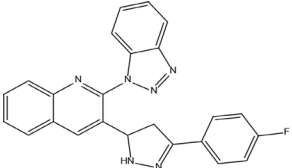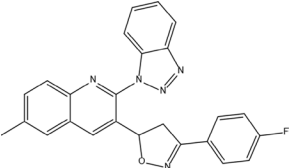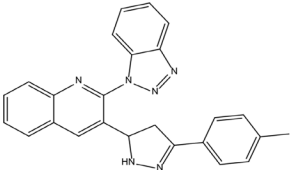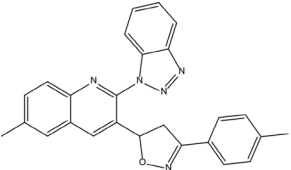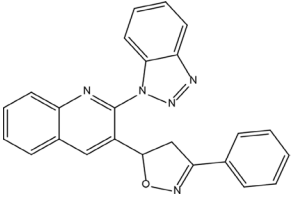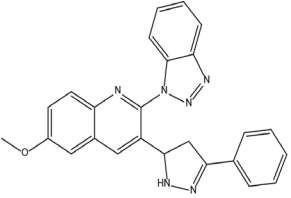
Salmonella typhi is a Gram-negative bacterial species responsible for typhoid fever infection, a disease that has caused significant morbidity and mortality globally, especially in developing nations (Akter *et al.* 2022; Stanaway *et al.* 2017). The increasing resistance of *Salmonella typhi* to many existing antibiotics is a threat to public health globally and has necessitated urgent search for newer drug candidates in the antibiotic drug development pipeline (Kariuki *et al.* 2010; Menezes *et al.* 2016; Peirano *et al.* 2014). In the quest for discovering novel drug candidates with unique mechanism of action against important enzymes of *Salmonella typhi*, some *in silico* studie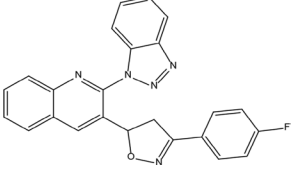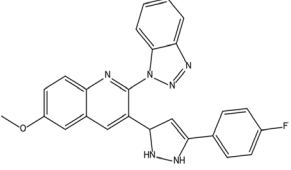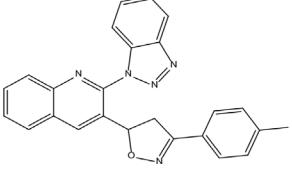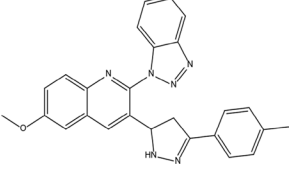s has been carried out of recent (Ameji *et al.* 2023a; 2023b; 2023c; Ameji *et al.* 2022; Anebi *et al.* 2021; Arunkumar *et al.* 2022; Qadir *et al.* 2018; Verma *et al.* 2020). However, this study is aimed at the discovery and design of highly potent and non-toxic quinoline-based antagonists of DNA gyrase of *Salmonella typhi*, an enzyme crucial to the replication processes in the bacterium.

METHODS

Retrieval of Data Set of Bioactive Ligands and Geometry Optimisation

A crucial step in CADD strategy is literature search for molecules with proven biological activities against a target pathogenic microbe. In this study, a data set of 18 anti-*Salmonella typhi* quinolines was retrieved from literature (Patel and Patel 2016). Table 1 presents their chemical structures and antibacterial activities. The chemical route of synthesis of the investigated quinoline derivatives is presented by Figure 1.

Table 1: Molecular structures and MIC values of the studied quinoline derivatives.

S/n	Structure	MIC (µg/mL)	S/n	Structure	MIC (µg/mL)
L1		250	L10		250
L2		200	L11		200
L3		250	L12		500
L4		200	L13		500
L5		250	L14		100
L6		500	L15		250

(continued on next page)

Table 1: (*continued*)

S/n	Structure	MIC (µg/mL)	S/n	Structure	MIC (µg/mL)
L7		250	L16		500
L8		100	L17		250
L9		200	L18		500
*	Ampicillin	250	*	Ciprofloxacin	100

Note: *reference antibiotics
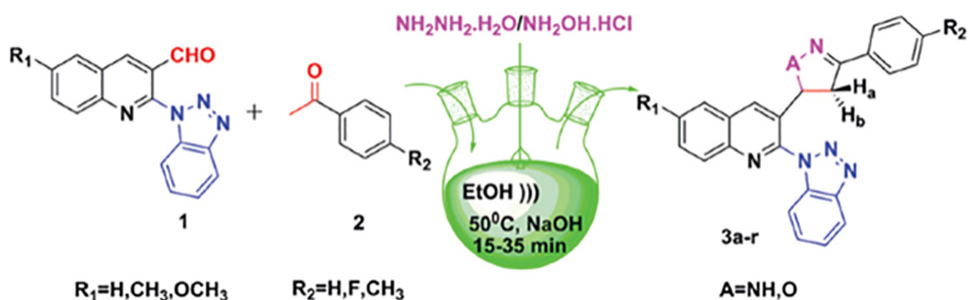
Figure 1: Synthetic route of the investigated Quinoline derivatives (Patel and Patel 2016).

Also, in order to mimic the natural forms of the bioactive ligands, their most stable conformations were obtained via geometry optimisation. The ChemDraw Ultra 12.0 software was used to draw the 2D structures of the ligands. The drawn ligands saved in cdx file format were exported unto Spartan 14.0 workspace where they were converted to 3D forms, pre-optimised using molecular mechanics force field (MMFF) and

finally by semi-empirical procedures (pm3). The optimised structures were subsequently saved in pdb file format for further investigations (Ameji *et al*. 2023a; 2023b; 2023c; Ameji *et al*. 2022).

Virtual Screening

Molecular docking technique was used to screen the bioactive quinoline ligands against DNA gyrase macromolecular target. The 3D structure of *Salmonella typhi*'s DNA gyrase (PDB code: 5ztj) was retrieved from protein data bank at www. rcsb. org/pdb. The water molecules, heteroatoms and co-crystallised ligands attached to the retrieved protease were removed using the Biovia Discovery Studio interface. The target protein was further processed via the addition of polar hydrogens and Kollman charges with the aid of AutoDock Vina tool v1.5.7. Finally, the docking calculation between the ligands and the target DNA gyrase was performed using PyRx software of AutoDock Vina tool by centering the Vina search space at X: −26.4401Å, Y: 23.0598Å and Z: 22.0813Å with dimensions of X: 51.6292Å, Y: 53.0044Å and Z: 51.8136Å (Ameji *et al*. 2023a; 2023b; 2023c; Ameji *et al*. 2022).

It is worthy of note that metal ions, especially divalent ions such as Mg^{2+} are crucial modulators of redox and non-redox catalytic activities in biological systems and account for one-third of enzyme mediated processes. They remove electron density from the ligand and cause polarisation of the substrate/cofactor reactive bonds, thereby increasing its electrophilic character. However, hydrogen bonding network in ligand/enzyme complexes often serve for catalytic activation and proper presentation of the reacting species (Sissi and Palumbo 2009). Thus, many molecular docking studies exclude the addition of metal ions such as Mg^{2+} during the Molecular docking simulations since the presence of hydrogen bond in the stable ligand/enzyme complex could also serves as modulator of catalytic activities (Aliye *et al*. 2021; Aoumeur *et al*. 2021; Jakhar *et al*. 2022; Sissi and Palumbo 2009).

Design of New Derivatives

One of the objectives of this study is to design analogues of the studied ligands with enhanced potencies against the target protease of *Salmonella typhi.* In achieving this, ligand with the best binding affinity among the virtually screened quinoline derivatives was selected as template molecule. Several derivatives were designed via structural adjustments. The derivatives were then screened against the DNA gyrase using the aforementioned procedures to ascertain their binding affinity against the target. Ligands with better potencies than the template were selected for further investigations (Ameji *et al*. 2023a; 2023b; 2023c; Ameji *et al*. 2022).

Assessment of Oral-Bioavailability

The Lipinski's rule of five and the Veber's rule were used to ascertain the drug-likeness (or oral bioavailability) of the template and the designed ligands. According to the Lipinski's rule, a drug must have its molecular weight (MW) ≤ 500, number of hydrogen bond donors (HBD) ≤ 5, octanol/water partition coefficient log P ≤ 5 and number of hydrogen bond acceptors (HBA) ≤ 10 for it to be orally bioavailable and violation of more than one of

these indices could translate to poor drug-likeness potentials of a ligand. Veber's rule, on the other hand stipulates that, for a drug to be orally bioavailable, the number of rotatable bonds (NRB) must be < 10 and topological polar surface area (TPSA) must be < 140 $Å^2$. The NRB, TPSA, MW, HBD, HBA and log P value of the most promising ligands were computed using the SwissADME (www.swissadme.ch/) online tool (Ameji *et al*. 2023a; 2023b; 2023c; Ameji *et al*. 2022).

Evaluation of ADMET Profiles

The high failure rates of drug candidates at the late stage of drug development have made prediction of pharmacokinetic and toxicity profiles of therapeutic ligands at the early stage of drug development a necessity. The template and the designed ligands were profiled for their gastrointestinal (GI) absorption, blood brain barrier (BBB) permeation, P-glycoprotein (P-gp+) substrate potentials and cytochrome-P450 enzymes inhibition using the SwissADME online server at http://www.swissadme.ch/index.php. Furthermore, Osiris DataWarrior V5.5.0 chemo-informatics programme was used to perform *in silico* toxicity assay on the selected bioactive ligands using the following toxicity endpoints; mutagenicity, reproductive effect and irritating effect (Ameji *et al*. 2023a; 2023b; 2023c; Ameji *et al*. 2022).

Quantum Mechanical Calculations

Generally, an ideal drug should be able to withstand physical and chemical degradation for a reasonable time frame to enable it exerts its therapeutic roles in the biological system. This unique characteristic is grossly influenced by the energies of its frontier molecular orbitals. These descriptors were computed using the Density Functional Theory (DFT) method of Spartan'14 software v1.1.4 at B3LYP hybrid functional and 6-31G** basis set. DFT method was chosen because of its computational efficiency and high accuracy in obtaining geometries, zero-point energy (ZPE) and frequencies (Ameji *et al*. 2023a; Miar *et al*. 2021).

Stabilities of the Ligands and Their Complexes with DNA Gyrase

The kinetic and thermodynamic parameters of the ligand/DNA gyrase complexes were computed using Equations 2 and 3, respectively, while those of the ligands alone were computed using Equations 5 and 6, respectively.

Quality Control

Quality control refers to the process and product-oriented strategies aimed at maintaining standard in research and development. Ciprofloxacin, an approved drug generally used in the treatment of *Salmonella typhi* infection, was docked against the target DNA gyrase using the procedures earlier described and the binding affinity value obtained was compared with those of the template and the designed ligands. Additionally, the drug-likeness, ADMET profile and stabilities of the standard antibiotic were also compared with those of the template and the designed ligands.

RESULTS

Molecular Docking Outcome

The results of the molecular docking based virtual screening of the investigated quinoline derivatives, the designed ligands and the standard ciprofloxacin antibiotic against DNA gyrase of *Salmonella typhi* are presented in Table 2. The Gibb's free energy change accompanying the LP interactions/binding affinity (ΔG) values were recorded in kcal/mol. Ligand 3 (L3) has the least ΔG value among the ligands. Thus, it formed the most stable complex with DNA gyrase and as such selected as template for designing more potent analogues. The 2D and 3D visual inspection results of interaction of L3 with the target macromolecule are presented in Figure 2.

Table 2: Binding affinity of ligand-macromolecule complex.

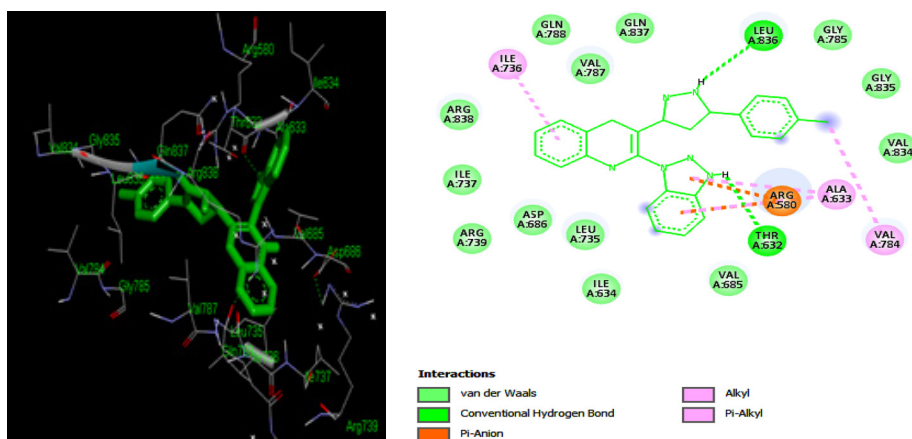| Ligand	ΔG (kcal/mol)	Ligand	ΔG (kcal/mol)
L1	−10.1	L12	−10.3
L2	−10.4	L13	−10.0
L3	−10.5	L14	−10.2
L4	−10.0	L15	−10.2
L5	−10.3	L16	−9.9
L6	−10.3	L17	−10.1
L7	−10.2	L18	−10.2
L8	−10.4	La	−10.7
L9	−10.4	Lb	−10.8
L10	−10.1	Lc	−7.7
L11	−10.3		

Figure 2: 3D and 2D diagrams of interaction of L3 with the active sites of DNA gyrase.

The Designed Analogues

In a bid to design more potent analogues, the template molecule (L3) was subjected to the following structural adjustments:

(i)   substitution of the hydrogen atom of benzo-1,2,3-triazole moiety with cyclopropenyl functional group

(ii)   substitution of the hydrogen atom of benzo-1,2,3-triazole moiety with cyclopropyl-1-enamine functional group

Molecular docking calculations revealed that out of the several derivatives formed, ligands La and Lb displayed better potencies against the target than the rest and are selected as the best newly designed ligands. The 2D chemical structures and IUPAC nomenclatures of La and Lb ligands are presented in Figure 3 while Figure 4 presents their mechanism of interaction with the active sites of the macromolecule.

A. Designed ligand (La)   B. Designed ligand (Lb)

C. Ciprofloxacin (Lc)

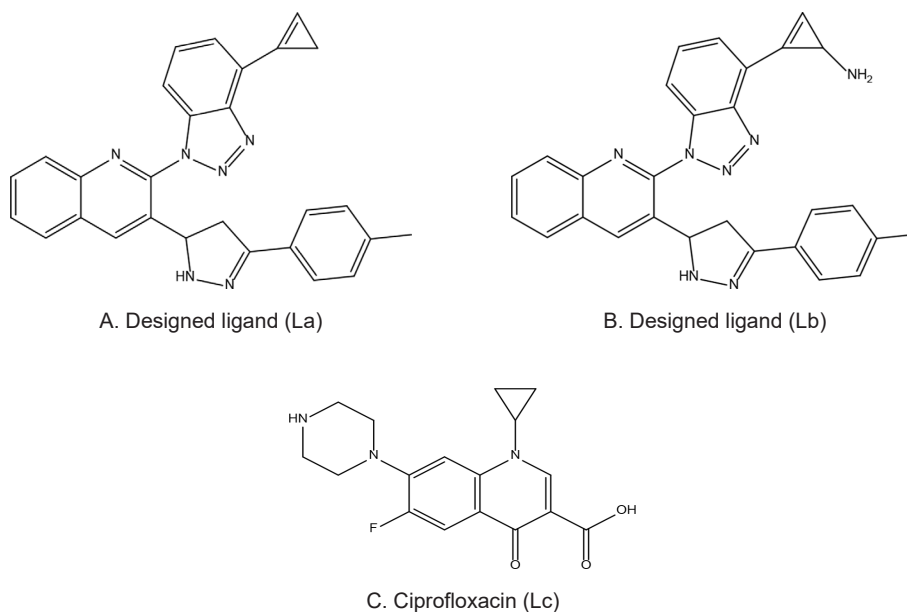**Figure 3:** Chemical structures of the designed ligands and ciprofloxacin.

A. 2-(4-(cycloprop-1-en-1-yl)-1H-benzo[d][1,2,3]triazol-1-yl)-3-(3-(p-tolyl)-4,5-dihydro-1H-pyrazol-5-yl)quinoline

B. 2-(1-(3-(3-(p-tolyl)-4,5-dihydro-1H-pyrazol-5-yl)quinolin-2-yl)-1H-benzo[d][1,2,3]triazol-4- yl)cycloprop-2-enamine

C. 1-cyclopropyl-6-fluoro-4-oxo-7-(piperazin-1-yl)-1,4-dihydroquinoline-3-carboxylic acid

A. La/DNA gyrase complex (−10.7 kcal/mol)

B. Lb/DNA gyrase complex (−10.8 kcal/mol)

C. Lc/DNA gyrase complex (−7.7 kcal/mol)
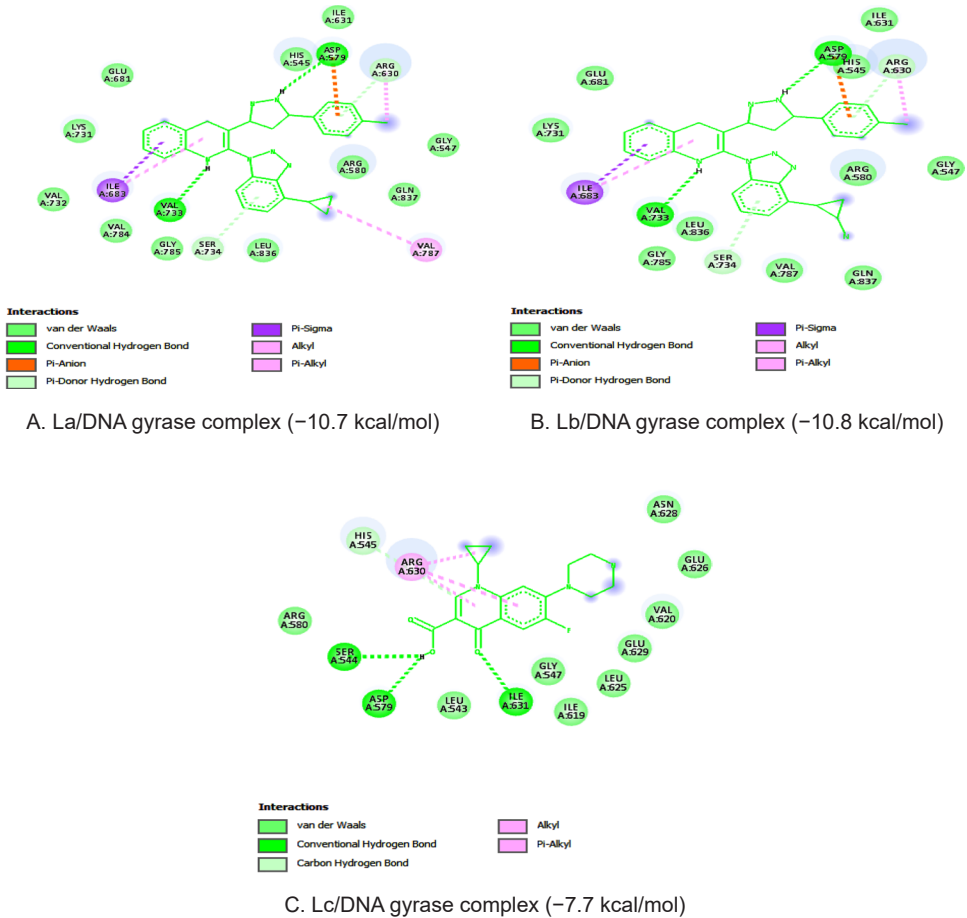
Figure 4: Interaction of the designed ligands and Ciprofloxacin with the target macromolecule in 2-dimensions.

Drug-likeness and ADMET Profiles

Oral bioavailability or drug-likeness properties of any therapeutic compound is a function of certain inherent physico-chemical properties of the compound. Table 3 presents the *in silico* drug-likeness assay of the template and the designed ligands. Also, their pharmacokinetic and toxicity profiles are presented in Table 4.

Table 3: Oral bioavailability profiles of the ligands.

Ligand rule	L3	La	Lb	Lc
Lipinski's	Yes	Yes	Yes	yes
HBA	4	4	5	5
HBD	1	1	2	2
MW (gmol^{-1})	404.5	442.5	457.5	331.34
cLogP$_{(o/w)}$	4.3	4.9	4.0	1.10
Veber's	Yes	Yes	Yes	Yes
NRB	3	4	4	3
TPSA (Å^2)	68.0	67.9	94.0	74.54

Notes: HBA = hydrogen bond acceptor; HBD = hydrogen bond donor; Mw = molecular weight; cLogP = consensus octanol water partition coefficient; NRB = number of rotatable bond; TPSA = topological polar surface area.

Table 4: ADMET profiles of ligands.

| Ligand	CYP450 substrate	GIA	P-gp$^+$	BBB	Mutagenicity	Irritant	Reproductive effect	Shape index
L3	Yes	High	Yes	Yes	High	None	None	0.48
La	Yes	High	No	Yes	High	None	None	0.47
Lb	Yes	High	Yes	No	High	None	None	0.49
Lc	Yes	High	Yes	No	High	None	None	0.50

Notes: GIA = gastrointestinal absorption; BBB = blood brain barrier penetration; P-gp$^+$ = P-glycoprotein substrate.

## Stabilities of the Ligands and their Complexes with DNA gyrase

The kinetic and thermodynamic stabilities of ligands and complexes are grossly influenced by descriptors such as the energies of LUMO and HOMO orbitals, global electrophilicity index (ω), global chemical hardness (η) and electronic chemical potential (μ) for the ligands as well as the dissociation constant (k_d) and binding or association constant (k_a) for the complexes. Table 5 presents the computed values of these descriptors. In addition, the molecular orbital diagrams of the ligands are presented in Figure 5.

Table 5: Descriptors of stabilities of the designed and the ciprofloxacin ligands.

Ligand	HOMO (eV)	LUMO (eV)	ΔE (eV)	μ (eV)	η (eV)	ω (eV)	ΔG (J/mol)	k_a (× 10^7)	k_d (× 10^{-8})
La	−5.37	−1.91	3.46	−3.64	1.73	3.83	−44769	7.04	1.42
Lb	−5.42	−1.97	3.45	−3.70	1.73	3.96	−45187	8.35	1.20
Lc	−5.63	−1.25	4.38	−3.44	2.19	2.70	−32217	0.04	226
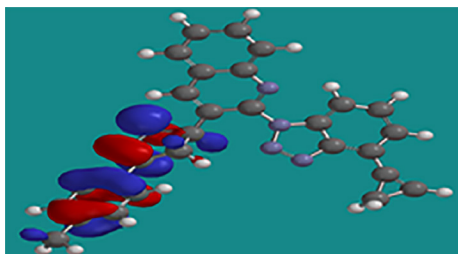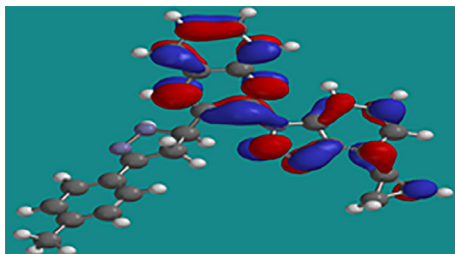
La: (A) HOMO (−5.37 eV)   (B) LUMO (−1.91 eV)
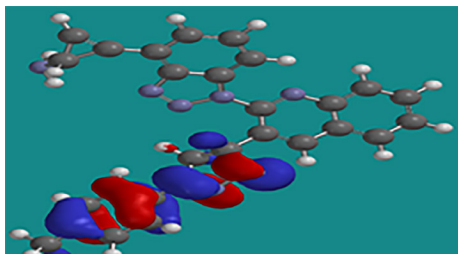
Lb: (A) HOMO (−5.42 eV)   (B) LUMO (−1.97 eV)

La: (A) HOMO (−5.63eV)   (B) LUMO (E= −1.25eV)

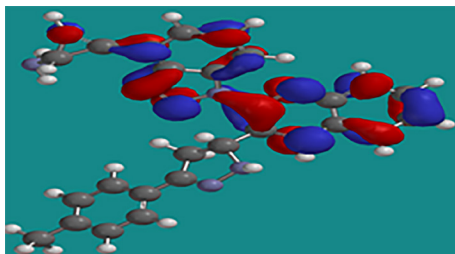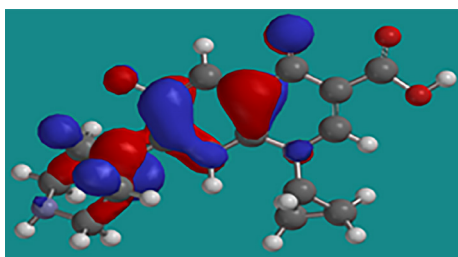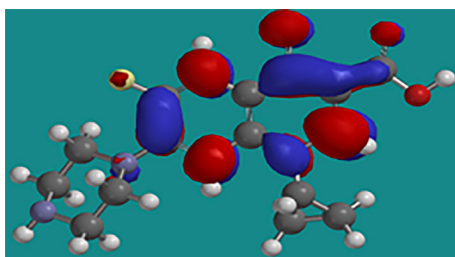**Figure 5:** DFT (B3LYP/ 6-31G**) derived frontier molecular orbital diagrams of La, Lb and Lc.

DISCUSSION

A major threat to public health is the alarming rate of multidrug resistance by pathogenic bacteria (*Salmonella typhi* inclusive). One way of confronting this dangerous trend is via constant search for novel drug candidates with unique mechanisms of action that is alien to the organisms. A major modus operandi of many antibiotics is the binding of the compounds to essential enzymes of the target microorganism, inhibiting the biochemical roles of the macromolecule and subsequently leading to inactivation or death of the organism. In search of newer drug candidates against *Salmonella typhi*, some bioactive quinoline based compounds were screened against DNA gyrase, an essential enzyme of the bacterium crucial to its replication processes. The results as displayed in Table 2 revealed that the ligands bind strongly and spontaneously with ΔG values ranging from −9.9 kcal/mol to −10.5 kcal/mol. L3 formed the most stable complex with the target

DNA gyrase with ΔG value of −10.5 kcal/mol and was selected as template molecule for designing more potent analogues; La and Lb with ΔG value of −10.7 kcal/mol and −10.8 kcal/mol, respectively. The investigated quinoline derivatives and the designed analogues could be more potent than the standard ligand (Lc) which binds with the target protease with ΔG value of −7.7 kal/mol.

Assessment of the mechanism of interaction of the ligands with the target macromolecule revealed that L3 binds to the active sites through electrostatic interaction (pi-anion) with ARG 580, conventional hydrogen bonds with LEU 836 and THR 632, and hydrophobic interactions (alkyl and pi-alkyl types) with ALA 633, VAL 784 and ILE 736 amino acid residues of the protease. Also, La binds to the amino acid residues of the target protease through an electrostatic (pi-anion) interaction with ASP 579; hydrophobic interactions with ARG 630, VAL 787 and ILE 683; two pi-donor hydrogen bonds with SER 734 and ARG 630; a pi-sigma interaction with ILE 683; and two conventional hydrogen bonds with ASP 579 and VAL 733. Furthermore, Lb interacted with the active sites of the target macromolecule via two alkyl (hydrophobic) associations with ILE 683 and ARG 630 amino acid side chains, a pi-anion (electrostatic) interaction with ASP 579, a pi-sigma interaction with ILE 683, two pi-hydrogen bonds with SER 734 and ARG 630, and two conventional hydrogen bonds with VAL 733 and ASP 579. The Lc on the other hand, binds to the target via hydrophobic interactions with ARG 630 amino acid side chain, and via formation of conventional hydrogen bonds with SER 544, ASP 579 and ILE 631.

By binding to the DNA gyrase target via hydrophobic interaction with ARG 630 and conventional hydrogen bond with ASP 579, Lb tends to display similar mechanism of interaction with the standard antibiotic, Lc. However, the template (L3) and the La ligands interact with the active sites of the target via mechanisms that are different from the standard antibiotic.

Drug-likeness measures the oral bioavailability potentials of a therapeutic ligand. It is a major assessment carried out at the early stage of drug development because many drugs are often administered through the oral route. In silico drug-likeness assay of the template and the designed ligands (Table 3) show that they obey both the Lipinski's rule of five and the Veber's rule like the reference ligand. Thus, the ligands could be regarded as orally bioavailable.

ADMET is concerned with the pharmacokinetic and toxicity properties of drug. It is concerned with the way the biological system interacts with therapeutic compounds for the duration of exposure and their possible adverse effects on the body. The ADMET profiles of the ligands (Table 4) revealed that they all possess excellent gastrointestinal absorption potentials and as such could be absorbed into the systemic circulation via the intestinal wall. The high gastrointestinal absorption of the ligands may be due to the presence of polar amine functional groups in the parent moiety. Also, the penetration of dissolve solute into the central nervous system is regulated by a tissue called blood brain barrier (BBB) (Bagchi *et al.* 2019; Miao *et al.* 2019). The result of ADMET evaluation (Table 4) reveals that L3 and La are substrate of BBB and are such could be BBB permeant, unlike Lb and Lc.

Another influencer of pharmacokinetic profile of drugs in the biological system is the permeability glycoprotein (P-gp[+]) whose primary function is the efflux of toxins and xenobiotic from the system. Substrates of P-gp[+] are prevented from entering the central nervous system and the epithelial cells from the systemic circulation and intestinal lumen, respectively (Chen *et al*. 2018). The pharmacokinetic data of the investigated ligands (Table 4) revealed that ligands L3, Lb and Lc are substrates of P-gp[+] unlike ligand Lb. Thus, the pharmacokinetic properties of the substrate ligands could be influenced by the efflux action of P-gp[+], unlike the non-substrate ligand (La).

Similarly, cytochrome P450 (CYP450) mono-oxygenase family also plays cardinal roles in the metabolism and biotransformation of drugs. Therapeutic ligands that inhibit all the isomers of CYP450 would have poor bioavailability and obnoxious toxicity profiles due to bioaccumulation (Zhao *et al*. 2021). The ADMET data (Table 4) revealed that all the ligands are substrates of CYP450 and as such could be easily metabolised, bio-transformed and excreted from the biological system.

The fate of a ligand with respect to it binding interaction with a target macromolecule is influenced by its shape. For this reason, the study of shape is fast gaining attention in molecular pharmacology. The analysis of the molecular shape index of the ligands (Table 4) revealed that they both possess shape index value of approximately 0.5, an optimum value for an ideal drug (Sander *et al*. 2015). It, thus, implies that the ligands are target specific (Kortagere *et al*. 2010). Though the designed ligands show high tendency of being mutagenic, they were however, found to be none-irritating and pose no threat to the reproductive system (Table 4).

For the investigated ligands to be excellent drug candidates, they ought to possess some level of stability to enable them to withstand physical and chemical degradation, a key requirement of an ideal drug. These properties are grossly dependent on the HOMO-LUMO energies of the ligand (Ameji *et al*. 2023a). DFT based quantum chemical calculations on the designed ligands (Table 5) revealed a HOMO-LUMO gap of 3.46eV and 3.45 eV for ligands La and Lb, respectively. These values are close to the 4.38 eV obtained for the reference antibiotic, Lc. The high HOMO-LUMO energies of the ligands connote their low chemical reactivity and high kinetic stability (Miar *et al*. 2021). The HOMO and LUMO orbitals of the ligands are presented in Figure 5.

A thermodynamic based descriptor known as global electrophilicity index (ω) is another descriptor of chemical reactivity of molecules. It measures the favourable energy change accompanying addition of electrons to a chemical system, i.e. energy decreases associated with flow of electrons from HOMO to the LUMO of molecules (Miar *et al*. 2021). A higher value of ω connotes good electrophilic behaviour and small value of the descriptor connotes good nucleophilic behaviour. Table 5 reveals ω value of 3.86 eV and 3.96 eV for La and Lb, respectively. When compared with Lc (ω = 2.70 eV), the designed ligands display better electrophilic behaviour and would bind with the target macromolecule with more favorable thermodynamic stabilities.

Also, the binding of La and Lb to the active sites of DNA gyrase was found to proceed via exergonic process with ΔG value of −44769 J/mol and −45187 J/mol, respectively (Table 5). When compared with the reference antibiotic, Lc which binds to the DNA gyrase with ΔG value −32217 J/mol, the designed ligands display more favourable thermodynamic stability of binding in agreement with the prediction of quantum mechanical calculations. Furthermore, La and Lb binds to the enzyme target with binding affinity (k_a) of 7.04×10^7 and 8.35×10^7, respectively. The ligand dissociation constant of 1.42×10^{-8} and 1.2×10^{-8} (k_d) were computed for La and Lb, respectively (Table 5). The astronomically higher values of k_a compared to k_d indicate high kinetic stability of the LP complexes in a mechanically perturbed biological system.

Practical Implications/Future Directions

The newly designed ligands; La and Lb has demonstrated immense inhibitory properties against the DNA gyrase of *Salmonella typhi* better than the quinolone based antibiotic used herein for quality control. Hence, synthesis and evaluation of their *in vitro* antimicrobial properties is highly recommended.

Limitations

This study is a theoretical research and as such further *in vitro* and *in vivo* studies are required in order to validate its findings.

CONCLUSION

The concepts of theoretical chemistry were used in this study to screen eighteen bioactive quinoline derivatives against DNA gyrase of *Salmonella typhi*. Molecular docking simulation of the ligands revealed that the interaction of the bioactive compounds with the active sites of the target macromolecule is exergonic. The most active ligand, L3, binds to DNA gyrase with ΔG value of -10.5 kcal/mol. Using L3 as template ligand, two more potent analogues; La and Lb were designed. La and Lb ligands were found to bind to the target enzyme with ΔG value of −10.7 kcal/mol and −10.8 kcal/mol; binding affinity constant (k_a) of 7.04×10^7 and 8.35×10^7; and dissociation constant (k_d) value of 1.42×10^{-8} and 1.2×10^{-8}, respectively. Also, DFT based quantum mechanical calculations on the designed ligands reveal that they possess excellent kinetic and thermodynamic stabilities. Furthermore, La and Lb ligands were found to have positive drug-likeness and outstanding pharmacokinetic profiles. The designed ligands tend to be consistent with all the validation protocols deployed in this study and as such could be recommended as novel drug candidates for treatment of *Salmonella typhi* induced salmonellosis.

ACKNOWLEDGEMENTS

REFERENCES

AKTER, T., CHAKMA, M., TANZINA, A. Y., RUMI, M. H., SHIMU, M. S. S. & SALEH, M. A. (2022) Curcumin analogues as a potential drug against antibiotic resistant protein, *β*-lactamases and L, D-transpeptidases involved in toxin secretion in *Salmonella typhi:* A computational approach, *Biomedinformatics*, 2: 77–100. https://doi.org/10.3390/biomedinformatics2010005

ALIYE, M., DEKEBO, A., TESSO, H., ABDO, T., ESWARAMOORTHY, R. & MELAKU, Y. (2021) Molecular docking analysis and evaluation of the antibacterial and antioxidant activities of the constituents of *Ocimum cufodontii*, *Scientific Reports*, 11: 10101. https://doi.org/10.1038/s41598-021-89557-x

AMEJI, J. P., UZAIRU, U., SHALLANGWA, G. A. & UBA, S. (2023a) Design, pharmacokinetic profiling, and assessment of kinetic and thermodynamic stability of novel anti-*Salmonella typhi* imidazole analogues, *Bulletin of the National Research Centre*, 47: 6. https://doi.org/10.1186/s42269-023-00983-5

AMEJI, J. P., UZAIRU, U., SHALLANGWA, G. A. & UBA, S. (2023b) Molecular docking simulation, drug-likeness assessment, and pharmacokinetic study of some cephalosporin analogues against a penicillin-binding protein of Salmonella typhimurium, *The Journal of Antibiotics*. https://doi.org/10.1038/s41429-023-00598-y

AMEJI, J. P., UZAIRU, U., SHALLANGWA, G. A. & UBA, S. (2023c) Obstructing *Salmonella typhi*'s virulence in eukaryotic cells through design of its SipB protein antagonists, *Journal of Taibah University Medical Sciences*, 18(4): e726–e736.

AMEJI, J. P., UZAIRU, U., SHALLANGWA, G. A. & UBA, S. (2022) Virtual screening of novel pyridine derivatives as effective inhibitors of DNA gyrase (GyrA) of *Salmonella typhi*, *Current Chemistry Letters*, 12: 1–16. https://doi.org/10.5267/j.ccl.2022.10.002

ANEBI, E., IBRAHIM, M. T., SHALLANGWA, G. A., ISYAKU, S., ABDULSALAM, S. & DANMALLAM, A. M. (2021) Molecular docking study, drug-likeness and pharmacokinetic properties (ADMET) prediction of some novel thiophene derivatives as *Salmonella typhi* Inhibitors, *Bayero Journal of Pure and Applied Sciences*, 14(2): 235–244. https://doi.org/10.4314/bajopas.v14i2.29

AOUMEUR, N., TCHOUAR, N., BELAIDI, S., OUASSAF, M., LANEZ, T. & CHTITA, S. (2021) Molecular docking studies for the identifications of novel antimicrobial compounds targeting of *Staphylococcus aureus*, *Morrocan Journal of Chemistry*, 9(1): 274–289.

ARUNKUMAR, M., MAHALAKSHMI, M., ASHOKKUMAR, V., ARAVIND, M. K., GUNASEELAN, S., MOHANKUMAR, V. *et al.* (2022) Evaluation of seaweed sulfated polysaccharides as natural antagonists targeting *Salmonella typhi* OmpF: Molecular docking and pharmacokinetic profiling, *Beni-Suef University of Basic and Applied Sciences*, 11: 8. https://doi.org/10.1186/s43088-021-00192-x

BAGCHI, S., CHHIBBER, T., LAHOOTI, B., VERMA, A., BORSE, V. & JAYANT, R. D. (2019) In-vitro bloodbrain barrier models for drug screening and permeation studies: an overview, *Drug Design, Development and Therapy*, 13: 3591–3605. https://doi.org/10.2147/DDDT.S218708

BATES, A. D. & MAXWELL, A. (2007) Energy coupling in type ii topoisomerases: Why do they hydrolyze ATP? *Biochemistry*, 46: 7929–7941.

BEHERA, S., MOHANTY, P., BEHURA, R., NATH, B., BARICK, A. K. & JALI, B. R. (2022) Antibacterial properties of quinoline derivatives: A mini-review, *Biointerface Research in Applied Chemistry,* 12(5): 6078–6092. https://doi.org/10.33263/BRIAC125.60786092

BEHFOROUZ, M., CAI, W., MOHAMMADI, F., STOCKSDALE, M. G., GU, Z., AHMADIAN, M. *et al*. (2017) Synthesis and evaluation of antitumor activity of novel N-acyllavendamycin analogues and quinoline-5, 8-diones, *Bioorganic & Medicinal Chemistry*, 15: 495–510. https://doi.org/10.1016/j.bmc.2006.09.039

CARPENTER, K. A., COHEN, D. S., JARRELL, J. T. & HUANG, X. (2018) Deep learning and virtual drug screening, *Future Medicinal Chemistry*, 10: 2557–2567. https://doi.org/10.4155/fmc-2018-0314

CARREGAL, A. P., MACIEL, F. V., CARREGAL, J. B., DOS REIS SANTOS, B., DA SILVA, A. M. & TARANTO, A. G. (2017) Docking-based virtual screening of Brazilian natural compounds using the OOMT as the pharmacological target database, *Journal of Molecular Modeling*, 23: 111. https://doi.org/10.1007/s00894-017-3253-8

CHEN, C., LEE, M., WENG, C. & LEONG, M. K. (2018) Theoretical prediction of the complex P-glycoprotein substrate efflux based on the novel hierarchical support vector regression scheme, *Molecules*, 23: 1820. https://doi.org/10.3390/molecules23071820

DEVI, R. V., SATHYA, S. S. & COUMAR, M. S. (2015) Evolutionary algorithms for de novo drug design—A survey, *Applied Soft Computing*, 27: 543–552. https://doi.org/10.1016/j.asoc.2014.09.042

DRLICA, K., HIASA, H., KERNS, R., MALIK, M., MUSTAEV, A. & ZHAO, X. (2009) Quinolones: Action and resistance updated, *Current Topics in Medicinal Chemistry*, 9(11): 981–998.

DUTKIEWICZ, Z. & MIKSTACKA, R. (2018) Structure-based drug design for cytochrome P450 family 1 inhibitors, *Bioinorganic Chemistry and Applications*, 2018: 3924608. https://doi.org/10.1155/2018/3924608

GHOLIZADEH, S. & RADMOGHADAM, K. (2014). Ultrasound-assisted the three-component synthesis of spiro[4H-pyrano[3,2-c]quinolin-4, 3_-indoline]-2_,5(6H)-diones in water, *Oriental Journal of Chemistry*, 29: 1637–1641. https://doi.org/10.13005/ojc/290450

JAKHAR, R., KHICHI, A., KUMAR, D., DANGI, M. & CHHILLAR, A. K. (2022) Discovery of novel inhibitors of bacterial DNA gyrase using a QSAR based approach, *ACS Omega*, 7: 32665−32678. http://pubs.acs.org/journal/acsodf

KARIUKI, S., REVATHI, G., KIIRU, J., MENGO, D. M., MWITURIA, J., MUYODI, J. *et al*. (2010) Typhoid in Kenya is associated with a dominant multidrug-resistant *Salmonella enterica* serovar typhi haplotype that is also widespread in Southeast Asia, *Journal of Clinical Microbiology*, 48: 2171–2176. https://doi.org/10.1128/JCM.01983-09

KOHANSKI, M. A., DWYER, D. J., HAYETE, B., LAWRENCE, C. A. & COLLINS, J. J. (2007) A common mechanism of cellular death induced by bactericidal antibiotics, *Cell*, 130(5): 797–810.

KORTAGERE, S., KRASOWSKI, M. D. & EKINS, S. (2009) The importance of discerning shape in molecular pharmacology, *Trends in Pharmacological Sciences*, 30(3): 138–147. https://doi.org/10.1016/j.tips.2008.12.001

KUMAR, M., SHARMA, K., SAMARTH, R. M. & KUMAR, A. (2010) Synthesis and antioxidant activity of Quinolinobenzothiazinones, *European Journal of Medicinal Chemistry*, 45; 4467–4472. https://doi.org/10.1016/j.ejmech.2010.07.006

LEELANANDA, S. P. & LINDERT, S. (2016) Computational methods in drug discovery, *Beilstein Journal of Organic Chemistry*, 12: 2694–2718. https://doi.org/10.3762/bjoc.12.267

LIMA, A. N., PHILOT, E. A., TROSSINI, G. H. G., SCOTT, L. P. B., MALTAROLLO, V. G. & HONORIO, K. M. (2016) Use of machine learning approaches for novel drug discovery, *Expert Opinion on Drug Discovery*, 11: 225–239. https://doi.org/10.1517/17460441.2016.1146250

LIMONGELLI, V. (2020) Ligand binding free energy and kinetics calculation in 2020. Wiley interdisciplinary reviews, *Computational Molecular Science*, 2020: 1–42. https://doi.org/10.1002/wcms.1455

LIU, S., ALNAMMI, M., ERICKSEN, S. S., VOTER, A. F., ANANIEV, G. E., KECK, J. L. *et al*. (2018) Practical model selection for prospective virtual screening, *Journal of Chemical Information and Modelling*, 59: 282–293. https://doi.org/10.1101/337956

MENEZES, G. A., HARISH, B. N., KHAN, M. A., GOESSENS, W. & HAYS, J. (2016) Antimicrobial resistance trends in blood culture positive *Salmonella paratyphi* A isolates from Pondicherry, India, *Indian Journal of Medical Microbiology*, 34: 222–227. https://doi.org/10.4103/0255-0857.180352

MIAO, R., XIA, L. Y., CHEN, H. H., HUANG, H. H. & LIANG, Y. (2019) Improved classification of blood-brain-barrier drugs using deep learning, *Scientific Reports*, 9: 8802. https://doi.org/10.1038/s41598019447734

MIAR, M., SHIROUDI, A., POURSHAMSIAN, K., OLIAEY, R. A. & HATAMJAFARI, F. (2021) Theoretical investigations on the HOMO–LUMO gap and global reactivity descriptor studies, natural bond orbital, and nucleus-independent chemical shifts analyses of 3-phenylbenzo[d]thiazole-2(3H)-imine and its para-substituted derivatives: Solvent and substituent effects, *Journal of Chemical Research*, 2021: 147–158

MUGUMBATE, G., MENDES, V., BLASZCZYK, M., SABBAH, M., PAPADATOS, G., LELIEVRE, J. *et al*. (2017) Target identification of *Mycobacterium tuberculosis* phenotypic hits using a concerted chemogenomic, biophysical, and structural approach, *Frontiers in Pharmacology*, 8: 681. https://doi.org/10.3389/fphar.2017.00681

NUNES, R. R., DA FONSECA, A. L., PINTO, A. C. D. S., MAIA, E. H. B., DA SILVA, A. M., VAROTTI, F. *et al*. (2019) Brazilian malaria molecular targets (BraMMT): Selected receptors for virtual high-throughput screening experiments, *Memorias Do Instituto Oswaldo Cruz*, 114: 1–10. https://doi.org/10.1590/0074-02760180465

PATEL, A. J. & PATEL, M. P. (2016) Synthesis and microbial studies of new pyrazoline/isoxazoline derivatives bearing quinoline moiety using ultrasound irradiation, *Indian Journal of Advances in Chemical Science*, 4(4): 409–420.

PEIRANO, G., VAN DER, B. I. J., FREEMAN, K. A., POIREL, L. J., NORDMANN, L., COSTELLO, P. *et al*. (2014) Characteristics of *Escherichia coli* sequence type 131 isolates that produce extended-spectrum lactamases: Global distribution of the H 30-Rx sublineage, *Antimicrobial Agents and Chemotherapy*, 58: 3762–3767. https://doi.org/10.1128/AAC.02428-14

QADIR, I. M., MUSHTAQ, H. & MOBEEN, T. (2018) *In-silico* study of potential carboxylic acid derivatives as D-glutamate ligase inhibitors in *Salmonella typhi*, *Kuwait Journal of Science*, 45(1): 100–107.

SANDER, T., FREYSS, J., von KORFF, M. & RUFENER, C. (2015) DataWarrior, an open source program for chemistry aware data visualization and analysis, *Journal of Chemical Information and Modelling*, 55(2). https://doi.org/10.1021/ci500588j

SISSI, C. & PALUMBO, M. (2009) Effects of magnesium and related divalent metal ions in topoisomerase structure and function, *Nucleic Acids Research*, 37(3): 702–711. https://doi.org/10.1093/nar/gkp024

SLIWOSKI, G., KOTHIWALE, S., MEILER, J., EDWARD, W. & LOWE, J. (2013) Computational methods in drug discovery, *Pharmacological Reviews*, 66: 334–395. https://doi.org/10.1124/pr.112.007336

SRIVASTAVA, R. (2021) Theoretical studies on the molecular properties, toxicity, and biological efficacy of 21 new chemical entities, *ACS Omega*, 6: 24891−24901. http://pubs .acs.org/journal/acsodf

STANAWAY, J. D., REINER, R. C., BLACKER, B. F., GOLDBERG, E. M., KHALIL, I. A., TROEGER, C. E. *et al*. (2019) The global burden of typhoid and paratyphoid fevers: A systematic analysis for the Global Burden of Disease Study 2017, *The Lancet Infectious Diseases*, 19: 369–381. https://doi.org/10.1016/S1473-3099(18)30685-6

SURABHI, S. & SINGH, B. (2018) Computer aided drug design: An overview, *Journal of Drug Delivery and Therapeutics*, 8: 504–509. https://doi.org/10.22270/jddt.v8i5.1894

TALELE, T. T., KHEDKAR, S. A. & RIGBY, A. C. (2010) Successful applications of computer aided drug discovery: Moving drugs from concept to the clinic, *Current Topics in Medicinal Chemistry*, 10: 127–41. https://doi.org/10.2174/156802610790232251

VERMA, A. K., DANYAYA, A. I., KUMAR, A., SHUAIBU, B. S., HAMZA, U. A., YAHAYA, N. L. *et al.* (2020) Virtual screening, molecular docking, and ADMET analysis of natural product library against cell invasion protein SipB from *Salmonella enterica* serotype typhi: *In silico* analysis, *Acta Scientific Pharmaceutical Sciences*, 4(8): 20–30.

WÓJCIKOWSKI, M., BALLESTER, P. J. & SIEDLECKI, P. (2017) Performance of machinelearning scoring functions in structure-based virtual screening, *Scientific Reports*, 7: 46710. https://doi.org/10.1038/srep46710

ZHAO, M., MA, J., LI, M., ZHANG, Y., JIANG, B., ZHAO, X. *et al.* (2021) Cytochrome P450 enzymes and drug metabolism in humans, *International Journal of Molecular Science*, 22: 12808. https://doi.org/10.3390/ijms222312808